10-28-1993

Interaction of Cationic Porphyrins with DNA

Ulrica Sehlstedt
Chalmers University of Technology

Pamela Carter
Syracuse University

Jerry Goodisman
Syracuse University

James C. Dabrowiak
Syracuse University

Seog K. Kim
Yeungnam University

Recommended Citation

Sehlstedt, U., Kim, S. K., Carter, P., Goodisman, J., Vollano, J. F., Norden, B., & Dabrowiak, J. C. (1994). Interaction of cationic porphyrins with DNA. Biochemistry, 33(2), 417-426.

Interaction of Cationic Porphyrins with DNA†

Ulrica Sehlstedt,‖ Seog K. Kim,‡ Pamela Carter,§ Jerry Goodisman,§ Jean F. Vollano,⊥ Bengt Nordén,*,‖ and James C. Dabrowiak*,§

Department of Physical Chemistry, Chalmers University of Technology, S-41296 Gothenburg, Sweden, Department of Chemistry, Yeungnam University, Kyoungsan City, Kyoung-buk, 712-749 Republic of Korea, Department of Chemistry, Syracuse University, Syracuse, New York 13244-4100, and Johnson-Matthey, Inc., West Chester, Pennsylvania 19380

Received July 20, 1993; Revised Manuscript Received October 28, 1993®

ABSTRACT: Utilizing linear dichroism (LD), circular dichroism (CD), and fluorescence energy transfer, the binding geometries of a series of Co^{3+}-porphyrins and their free ligands were examined. The compounds studied were Co–*meso*-tetrakis(*N*-methylpyridinium-4-yl)porphyin (CoTMPyP) and its free ligand (H_2-TMPyP), Co–*meso*-tetrakis(*N*-*n*-butylpyridinium-4-yl)porphyrin (CoTBPyP) and its free ligand (H_2TBPyP), and Co–*meso*-tetrakis(*N*-*n*-octylpyridinium-4-yl)porphyrin (CoTOPyP). The two non-metalloporphyrins exhibit negative LD, having angles of roughly 75° relative to the DNA helix axis. They also display negative CD and a significant contact energy transfer from the DNA bases. On the other hand, the three metalloporphyrins display orientation angles of roughly 45° between the porphyrin plane and the helix axis of DNA. Furthermore, they exhibit positive CD and no contact energy transfer from DNA bases. These observations show that the metalloporphyrins are not intercalated whereas non-metalloporphyrins having four freely rotating *meso*-aryl groups intercalate between the base pairs of DNA. In the presence of $KHSO_5$, the cobalt porphyrins cleave closed circular PM2 DNA in a single strand manner, *i.e.*, a single activation event on the porphyrin leads to a break in one of the DNA strands. A kinetic analysis of the cleavage data revealed that cleavage rates are in the order CoTMPyP > CoTBPyP > CoTOPyP with the difference being due to different DNA affinities rather than differences in cleavage rate-constants. Based on these and earlier observations, the metalloporphyrins appear bound to a partially melted region of DNA.

Water-soluble cationic porphyrins bind to DNA. The pioneering work of Fiel (1989) and Pasternack and their co-workers (Pasternack & Gibbs, 1989) established that the binding mechanism could be modulated by the nature of the metal ion and the size and location of the substituent groups on the periphery of the porphyrin. Generally, the free bases and square planar complexes such as those with Ni^{2+} and Cu^{2+} intercalate between the base pairs of DNA. For complexes having axially bound ligands such as those with Mn^{3+}, Fe^{3+}, and Co^{3+} or those with bulky substituents located on the periphery of the structure, intercalation is blocked and "outside" binding occurs. Recent studies show that intercalation versus outside binding may also be influenced by the charge on the porphyrin core (Marzilli *et al.*, 1992; Kuroda *et al.*, 1990).

The most extensively studied DNA binding porphyrin is *meso*-tetrakis(*N*-methylpyridinium-4-yl)porphyrin, H_2TMPyP (Figure 1). As was originally demonstrated by Fiel and co-workers (Fiel *et al.*, 1982), FeTMPyP can be chemically activated to produce breaks in DNA. Additional work by the groups of Dabrowiak and co-workers (Raner *et al.*, 1989; Ward *et al.*, 1986a,b) and of Bernadou and Meunier and their co-workers (Fouguet *et al.*, 1987; Pratviel *et al.*, 1989; Bernadou *et al.*, 1989) established that M–TMPyP where M is Fe^{3+}, Mn^{3+}, and Co^{3+} can be activated with a variety of oxidizing agents to produce breaks in DNA. Analysis of cleavage products using the sequencing methods showed that the preferred binding site is a triplet containing only adenine and thymine. In the presence of the oxidizing agent $KHSO_5$, MnTMPyP can be used as a footprinting agent for AT-specific drugs (Dabrowiak *et al.*, 1989). Also, the temperature dependence of the compound's cleavage specificity suggests that it may be a probe for low-melting regions of DNA (Raner *et al.*, 1988, 1989).

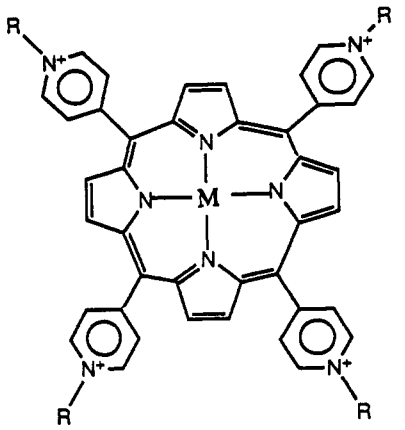

M	R	
Co^{+3}	$-CH_3$	Co TMPyP
Co^{+3}	$-(CH_2)_3-CH_3$	Co TBPyP
Co^{+3}	$-(CH_2)_7-CH_3$	Co TOPyP
$2H^+$	$-CH_3$	H_2 TMPyP
$2H^+$	$-(CH_2)_3-CH_3$	H_2 TBPyP

FIGURE 1: Structures of the cobalt porphyrins and the free ligands. The cobalt porphyrins have axial ligands (Cl^-, ^-OH, H_2O) above and below the porphyrin plane.

† Support to P.C. from the National Science Foundation, Research Experience for Undergraduates [CHEM-9200501], is greatly acknowledged.

* To whom correspondence should be addressed.
‖ Chalmers University of Technology.
‡ Yeungnam University.
§ Syracuse University.
⊥ Johnson-Matthey, Inc.

® Abstract published in *Advance ACS Abstracts,* December 15, 1993.

0006-2960/94/0433-417$04.50/0

A detailed study by Bernadou and Meunier and their co-workers (Pratviel *et al.*, 1991; Gasmi *et al.*, 1991; Pitié *et al.*, 1992) showed that MnTMPyP cleaves DNA from its minor grove. For calf thymus DNA, the activated oxo species attacks C1′-H, which is located deep within the minor groove. For oligonucleotides, cleavage selectivity occurs on the 3′ sides of three contiguous AT base pairs. The oxo species primarily hydroxylates the 5′ carbon of deoxyribose, located in the minor groove, ultimately causing a break which leaves a 3′-phosphate and a 5′-aldehyde at the scission site.

In addition to chemical activation, porphyrins can be photochemically activated to attack biological molecules. For example, photodynamic therapy (Berg *et al.*, 1978; Diamond *et al.*, 1977) very likely involves damage to membranes through the photoinduced production of singlet oxygen. Although the details of the cleavage mechanisms are not known, studies with plasmid DNA indicate that certain metalloporphyrins can cause both single- and double-strand breaks in DNA (Praseuth *et al.*, 1986; Fiel *et al.*, 1981).

The structure of the porphyrin–DNA complex has been characterized using a variety of physical techniques. Extensive NMR, equilibrium dialysis, flow dichroism, and viscometry measurements on oligomeric and polymeric DNA's by Marzilli, Wilson, and their co-workers [for an excellent review see Marzilli (1990); Strickland *et al.*, 1990] have supported the original proposal that porphyrins intercalate into GC-rich regions and that they bind in an outside manner at AT sites (Fiel, 1989). Geacintov *et al.* (1987) found that H_2TMPyP, which intercalates, is aligned perpendicualr to the DNA helix axis, while ZnTMPyP, which binds outside to AT sites (Fiel, 1989; Ward *et al.*, 1986a,b), lies at an angle of 62–67° relative to the helix axis. These structural features are consistent with the results of molecular modeling and energy minimization studies on dinucleotide (Ford *et al.*, 1987) and oligonucleotide (Hui *et al.*, 1990) complexes of H_2TMPyP.

In an attempt to learn more about the manner in which cationic porphyrin complexes interact with DNA, especially those which bind outside in the minor groove, we characterized the DNA binding and cleavage properties of the cobalt porphyrins shown in Figure 1. The porphyrins possess four alkylated pyridine residues having methyl (H_2TMPyP), *n*-butyl (H_2TBPyP), and *n*-octyl (H_2TOPyP) groups. We reasoned that if the DNA helix were intact at the site of binding, bulky substituent groups on the periphery of the porphyrin could alter the structure of the porphyrin–DNA complex. Changes in structure could in turn be detected by alterations in the angle that the porphyrin plane makes with the helix axis and/or changes in rates associated with porphyrin cleavage of DNA.

When bound to calf thymus DNA, the cobalt porphyrins exhibit induced CD effects that are similar in sign and magnitude, suggesting a common binding mode for all compounds. Furthermore, linear dichroism (LD) shows that the porphyrin plane is oriented at an angle of 42–45° relative to the helix axis, indicating that the compounds are "end-on" bound. In the range 220–300 nm, LD also shows that DNA molecules having the bound cobalt porphyrins are difficult to orient along the flow lines. These observations sharply contrast with those of the non-metal porphyrins H_2TMPyP and H_2-TBPyP, which have induced CD effects and orientation angles consistent with intercalation into DNA. In the presence of $KHSO_5$, the coblat porphyrins cleave the closed circular form of PM2 DNA in a single-strand manner, *i.e.*, a single activation event on the porphyrin leads to a break in one of the DNA strands. A kinetic analysis shows that the apparent cleavage rates for conversion of form I DNA to form II DNA are in the order CoTMPyP > CoTBPyP > CoTOPyP. This is likely caused by differences in DNA affinities rather than by differences in cleavage rate constants. These results, and those of earlier work, support a model having the metalloporphyrin in a partially melted region of DNA. The unmetallated analogues, on the other hand, intercalate into DNA.

MATERIALS AND METHODS

Materials. The PM2 DNA was used as obtained from Boehringer Mannheim Biochemical. Oxone, $KHSO_5$, was purchased from Aldrich Chemical Co. Calf thymus DNA, CT DNA (source Sigma Chemical Co.), was dissolved in 1 mM EDTA, 100 mM NaCl, and 5 mM cacodylic buffer at pH 7.0 by exhaustive stirring at 4 °C. The DNA solution was dialyzed against 5 mM cacodylic buffer with 20 mM NaCl at 4 °C, and the buffer was changed six times with 5-h intervals. Afterwards, the hypochromicity of DNA at 260 nm was found to be 40%. All of the synthesized compounds had acceptable combustion analytical data.

(CoTMPyP)Cl_5·7NaCl·13H_2O. To 11 g of H_2TMPyP-(TOS)$_4$ (Strem Chemical Co.) in 225 mL of water was added 10 g of Dowex 1 anion-exchange resin in the chloride form. After being stirred for 1 h, the resin was removed by filtration, and 18 g of $CoCl_2$·6H_2O was added to the filtrate. The solution was refluxed for 14 h and cooled to room temperature, and its volume was reduced *in vacuo*. The addition of excess aqueous $NaClO_4$ resulted in the precipitation of the perchlorate salt of the complex. The ClO_4^- counter-ion was exchanged for Cl^- using Dowex 1 in the chloride form, and the product was recovered by freeze drying. The yield was 7.2 g.

(CoTBPyP)BF_5·6H_2O. To 8 g of H_2TBPyP(BF_4)$_4$ (Strem Chemical Co.) in 500 mL of water was added 15 g of Dowex 1 anion-exchange resin in the chloride form. After 1 h the resin was removed by filtration, and 18 g of $CoCl_2$·6H_2O was added to the filtrate. After being refluxed for 6 h, the solution was cooled and excess aqueous $NaBF_4$ added. The product, as BF_4^- salt, was recovered by filtration and was air-dried. The yield was 7.2 g.

H_2TOPyPCl_4. A total of 158 g (2 mol) of pyridine was added to 0.5 mol of octanol. The reaction mixture was placed in an ice bath, and 105 g (0.55 mol) of *p*-toluenesulfonyl chloride was slowly added so that the temperature never exceeded 12 °C. The reaction mixture was then stirred for 3 h at a temperature around 15 °C, after which time it was diluted with 300 mL of HCl in 1 L of ice water. Then the product was extracted from the reaction with ether. The ether was then removed *in vacuo*, and 90 g of octyl tosylate was obtained.

A total of 50 g of octyl tosylate was added to 500 mL of DMF followed by 6 g of tetra(4-pyridyl)porphine. The reaction mixture was refluxed for 10 h. The volume of DMF was reduced by evaporation to 80 mL, and 200 mL of water was added. After being filtered, the semisolid was stirred in a cold water/5% acetone mixture, filtered again, and air-dried. Then the counter-ion was changed to chloride using a Dowex 1 ion-exchange resin. The yield was 8 g.

(CoTOPyP)Cl_5·8H_2O. The free ligand H_2TOPyPCl_4, 4g, in a small amount of acetone was added to 500 mL of water containing 15 g of $CoCl_2$·6H_2O. The reaction was refluxed for 6 h. After the mixture cooled, excess aqueous $NaClO_4$ was added to induce crystallization. The ClO_4^- counter-ion was converted to the chloride form in the manner described for the previous compounds.

Cleavage Reactions. The cleavage reactions involving DNA were carried out in a total volume of 9 μL at room temperature. To 4 μL of the appropriate porphyrin solution in 10 mM Tris-HCl, pH 8.0, was added 1 μL of PM2 DNA (0.25 μg/μL) in water. Following the equilibration of each porphyrin–DNA solution, 4 μL of freshly prepared aqueous 10 mM oxone (potassium monopersulfate) was added to activate the metalloporphyrin. The final concentrations of various components in the reaction mixture were as follows: PM2 DNA, 46 μM base pairs; oxone, 4.4 mM; Tris-HCl, 4.4 mM. The final concentration of CoTMPyP in the various reactions, which is also the order in the wells of the gel from left to right, was, 0, 9.2×10^{-8}, 0, 9.2×10^{-8}; 1.15, 1.54, 2.31, 3.08, 4.63, 6.17, 9.26×10^{-7}; 1.85, 4.63×10^{-6}; and 4.63×10^{-5} M. The concentrations of CoTBPyP and CoTOPyP were 0, 0, 9.2×10^{-8}, 9.2×10^{-8}; 1.15, 1.54, 2.31, 3.08, 4.63, 6.17, 9.26×10^{-7} M; 1.85, 4.63, and 9.27×10^{-6} M. The reaction was allowed to proceed for 15 min, at which time 4 μL of 10 mM sodium dodecyl sulfate (SDS) was added to terminate the reaction. Finally, 2 μL of a nondenaturing gel-loading buffer containing 0.25% bromophenol blue, 0.25% xylene cyanol, and 50% glycerol was added to each solution. The solutions were then loaded onto a 1% (w/vol) horizontal agarose gel and electrophoresed at a constant voltage using tris–acetate (TAE) buffer.

After electrophoresis, the gel was soaked in a solution of ethidium bromide (10 mg/mL) in 400 mL of water for approximately 30 min. While resting on a UV transilluminator, the gel was photographed, and both a positive and a negative were obtained. The negative was "fixed" in an aqueous solution containing sodium sulfite and then rinsed several times in water. The negatives were then scanned by a Molecular Dynamics microdensitometer, Model 300A, in order to obtain the intensity of each spot appearing on the gel.

Analysis of DNA Cleavage. Due to non-uniform intensity of the transilluminator, the scanned intensities were corrected in the previously described manner (Kishikawa, 1991). Because of its superhelical nature, the ability of form I DNA to stain under saturated ethidium bromide conditions was less than that of forms II and III DNA: the earlier determined factor of 0.8 was used to multiply calculated intensities of form I DNA (Bauer & Vinograd, 1968).

The kinetic scheme assumed, with I, II, and III representing supercoiled, open circular, and linear PM2 DNA, respectively, was as follows:

$$\mathrm{I} \xrightarrow[k_1]{} \mathrm{II} \xrightarrow[k_2]{} \mathrm{III} \xrightarrow[k_3]{} \text{products}$$

Assuming all reactions to be first order in the concentration of DNA, expressions for the concentrations of the three forms as a function of time are easily derived:

$$[\mathrm{I}] = C_0 e^{-k_1 t} \tag{1}$$

$$[\mathrm{II}] = \frac{k_1 C_0}{k_2 - k_1} e^{-k_1 t} + \left(N_0 - \frac{k_1 C_0}{k_2 - k_1} \right) e^{-k_2 t} \tag{2}$$

$$[\mathrm{III}] = \alpha e^{-k_1 t} + \beta e^{-k_2 t} + (L_0 - \alpha - \beta) e^{-k_3 t} \tag{3}$$

Here the initial concentrations of I, II, and III are C_0, N_0, and L_0, respectively, and

$$\alpha = k_1 k_2 C_0 (k_2 - k_1)^{-1} (k_3 - k_1)^{-1} \tag{4}$$

$$\beta = k_2 \left(\frac{-k_1 C_0}{k_2 - k_1} + N_0 \right) (k_3 - k_2)^{-1} \tag{5}$$

The processes are actually second-order, but may be treated as pseudo-first-order because the concentration of porphyrin does not change with time during a digest. Each rate constant, k_i, in these pseudo-first-order processes is actually a product of a second-order rate constant k_i' and the concentration of porphyrin. Because rate constants always appear multiplied by time and porphyrin concentration, changing time t is equivalent to changing porphyrin concentration.

In the expressions for [I], [II], and [III], $e^{-k_1 t}$ is replaced by $\exp(-k_1' c_p \tau)$, where c_p is the porphyrin concentration and the value of t is fixed in the experiments at τ, the digest time, which is always 10 min. Other exponential terms are replaced similarly. The coefficients of the exponential terms involve ratios of rate constants, so they remain unchanged except that k_i' replaces k_i. Spot intensities on the gels are proportional to concentrations of DNA. By fitting the intensities for forms I, II, and III as a function of porphyrin concentration to the above expressions, one can extract values for the six parameters C_0, N_0, L_0, $k_1'\tau$, $k_2'\tau$, and $k_3'\tau$.

The fact that the concentration of form III (linear) DNA is too small to observe implies that L_0 is small and that [I] + [II] $\approx C_0$. To verify the constancy of [I] + [II], we form for each porphyrin concentration c_p. $S = (1/0.8)$ times the intensity of the spot corresponding to form I DNA plus the intensity of the spot corresponding to form II DNA. S, which should be proportional to [I] + [II], is fitted to polynomials in c_p. The mean-square deviation between the polynomial and the value of S does not decrease much in going from zero-order to first-order to second-order polynomials, indicating that S is indeed constant.

The value of the constant was used to normalize the data, *i.e.*, all intensities for each concentration of, for example, CoTMPyP were multiplied by the average value of S divided by the corresponding value of S for that concentration. This compensates for dilution errors, loading errors, and unequal illumination of different gel lanes by the transilluminator. The resulting correcting intensity data were used in the kinetic analysis.

Linear Dichroism. Linear dichroism (LD) on flow-aligned DNA was measured in a couette cell of Wada type (Wada & Kozawa, 1964) on a Jasco J500A spectropolarimeter as described earlier (Nordén & Tjerneld, 1976; Nordén & Seth, 1985; Nordén *et al.*, 1992). The reduced linear dichroism (LD^r), i.e., the ratio between LD and isotropic absorbance, A_{iso}, at a given wavelength, λ, is related to the angle, α, between the light-absorbing transition dipole and the local helix axis of DNA according to eq 6, where S is an orientation function such that $S = 1$ for DNA perfectly aligned parallel to the flow lines and $S = 0$ for isotropic orientation (Nordén *et al.*, 1992):

$$LDr(\lambda) = LD(\lambda)/A_{iso}(\lambda) = \frac{3S}{2}(3\cos^2\alpha - 1) \tag{6}$$

An effective value of α was calculated from the maximum LD^r observed for the in-plane polarized $\pi \rightarrow \pi^*$ transitions in the Soret and visible porphyrin absorption bands by comparison with the LD^r observed for the DNA bases using an effective α value of 86° at 260 nm (Matsuoka & Nordén, 1983).

Large α values (80–90°) are indicative of intercalation whereas small values, such as 40–50°, are rather consistent with groove binding and, in any case, exclude intercalation binding geometries. In the present case, as a result of degenerate in-plane polarization of $\pi \rightarrow \pi^*$ transitions of the porphyrin chromophores, the apparent α value corresponding to a tilt of the porphyrin plane by an angle β will be larger than the tilt (*i.e.*, $\alpha > \beta$). The tilt is obtained by replacing $\cos^2\alpha$ in eq 6 by $(1/2)\cos^2\beta$ (Härd & Nordén, 1986).

Energy Transfer. Fluorescence energy transfer is the transfer of electronic excitation energy from a donor to an acceptor. Since the first report of contact energy transfer from DNA bases to bound ligands by Le Pecq and Paoletti in 1967, this technique has been used frequently in DNA–ligand interaction studies. In our work, the technique was applied to assess the interaction between the porphyrin chromophore and the DNA bases.

The ratio between the quantum yield of the bound porphyrin, with excitation in the UV spectral region of nucleic acids ($\phi(\lambda)$), the quantum yield with excitation at 310 nm ($\phi(310)$) was calculated as (Le Pecq & Paoletti, 1967):

$$\frac{\phi(\lambda)}{\phi(310)} = \left(\frac{I(\lambda)}{I(310)}\frac{\epsilon(310)}{\epsilon(\lambda)}\right)_b \left(\frac{I(310)}{I(\lambda)}\frac{\epsilon(\lambda)}{\epsilon(310)}\right)_f \quad (7)$$

where I denotes the fluorescence intensity and ϵ denotes absorption. The indices b and f refer to bound and free ligands, respectively. λ = 310 nm was chosen as the normalization wavelength because of the very low absorption of DNA in this region of the spectrum.

The fluorescence spectra were recorded on an Aminco SPF-500 spectrofluorometer in the quantum corrected mode. In order to avoid second-order spectra, a 375-nm cutoff filter was utilized. The excitation spectra were recorded for an emission wavelength of 660 nm and band width of 40 nm. All spectra were corrected for inner filter effects.

RESULTS AND ANALYSIS

Absorption Spectra. The interaction of CoTMPyP, CoTBPyP, CoTOPyP, H_2TMPyP, and H_2TBPyP with CT DNA was monitored with visible absorption spectroscopy. The absorption spectra of the free porphyrins and the porphyrins bound to CT DNA are depicted in Figure 2. The increase in absorbance in the 220–280-nm region upon addition of the porphyrins is attributable to the porphyrin molecules (Geacintov *et al.*, 1987). For all the porphyrins, binding to DNA leads to a substantial red-shift of the Soret maximum. For the free ligands, H_2TMPyP and H_2TBPyP hypochromicity in the Soret band is 50 and 35%, respectively, while CoTMPyP, CoTBPyP, and CoTOPyP show smaller hyperchromicities in the Soret band of 7, 14, and 6%, respectively.

Induced CD. The porphyrins and metalloporphyrin derivatives considered here do not display circular dichroism (CD) spectra in the absence of nucleic acids, but CD spectra are induced for the various porphyrins with DNA. A number of representative spectra are shown in Figure 3. All of the metalloporphyrin derivatives examined display positive CD spectra when bound to CT DNA. This profile is similar to that of di-*tert*-butylproflavin (Dalgleish *et al.*, 1972) which does not intercalate and has a specificity for AT-rich DNA (Müller *et al.*, 1973). Conversely, H_2TMPyP displays a negative CD spectrum, and the induced CD spectrum of H_2TBPyP is composed of both positive and negative components, where the positive band has a smaller ellipticity than the negative band. This spectrum is similar to the visible CD spectrum observed for the proflavin complex with DNA (Dalgleish *et al.*, 1969). Proflavin is a known intercalator in both GC and AT sites.

LD and LD′. The LD spectra of DNA complexes of all the porphyrins examined are depicted in Figure 4a–e. The LD signals at long wavelength (300–650 nm) for all the DNA–porphyrin complexes are negative, which indicates that the transition moments that are oriented within the planes of the molecules (Weiss *et al.*, 1972) are on the average tilted more perpendicular than parallel to the flow lines (Wada & Kozawa,

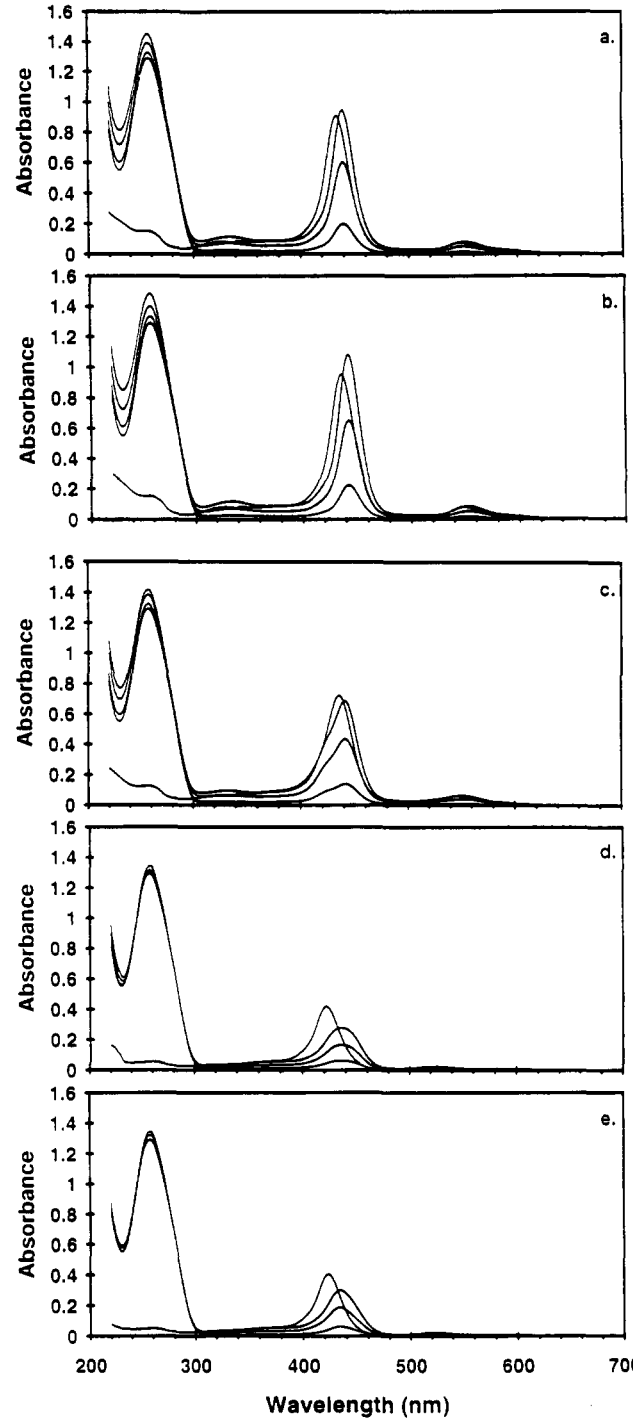

FIGURE 2: Absorption spectra of CoTMPyP (a), CoTBPyP (b), CoTOPyP (c), H_2TMPyP (d), and H_2TBPyP (e); free (1 μM) and bound to CT DNA. The R values, [porphyrin]/[DNA base], are 0.000, 0.002, 0.006, and 0.010 from bottom to top in the Soret region. DNA concentration is 100 μM, and the optical path length is 10 mm.

1964; Nordén & Tjerneld, 1976). However, as an effect of degeneracy or near-degeneracy of electronic states in the effectively 4-fold symmetric metal porphyrins, the apparent angle α, as obtained from eq 6, does not correspond to the angle the plane of the chromophore makes to the helix axis. The true angle, β, is instead obtained as the solution to $\cos^2 \beta = 2 \cos^2 \alpha$ (Materials and Methods). In Table 1 the corresponding tilts, β, are given. Clearly, whereas the metal-free porphyrins show a perpendicular binding geometry, consistent with intercalation, the metal porphyrins bind to DNA at angles close to the pitch of the minor groove, a

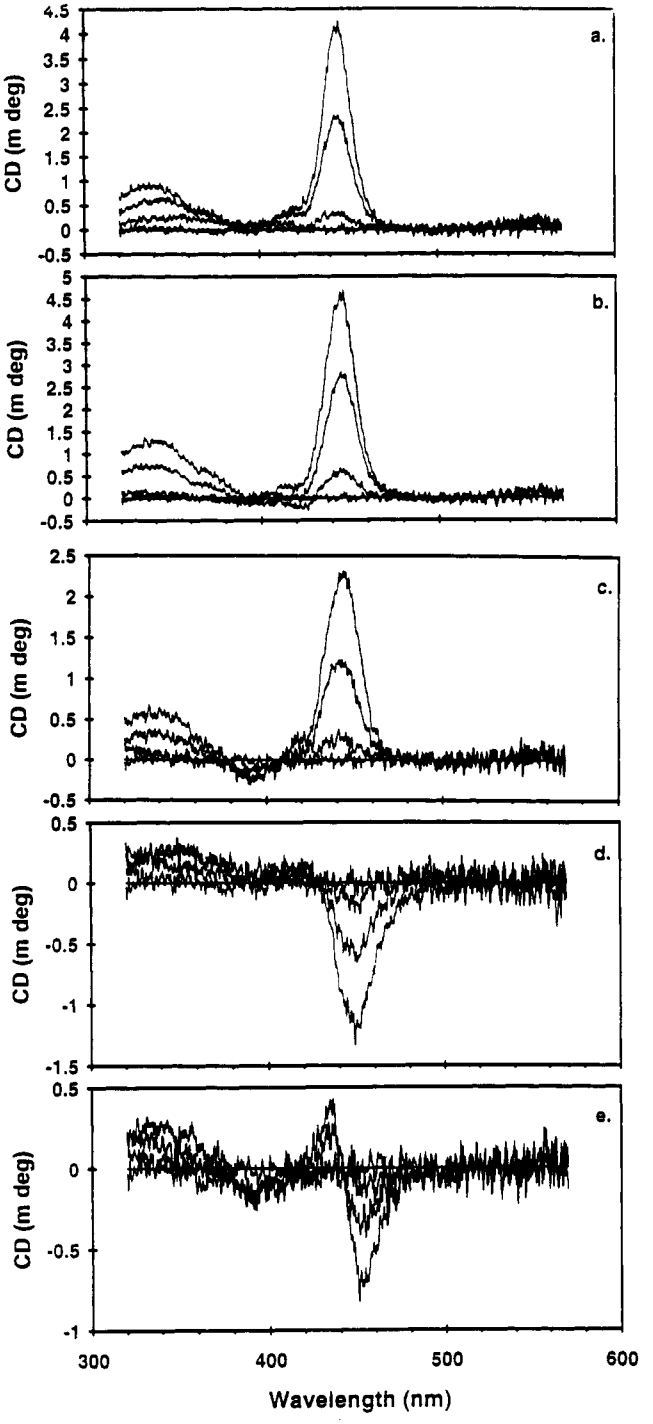

FIGURE 3: CD spectra of CT DNA complexed to CoTMPyP (a), CoTBPyP (b), CoTOPyP (c), H_2TMPyP (d), and H_2TBPyP (e). Concentrations and path length are the same as in Figure 2.

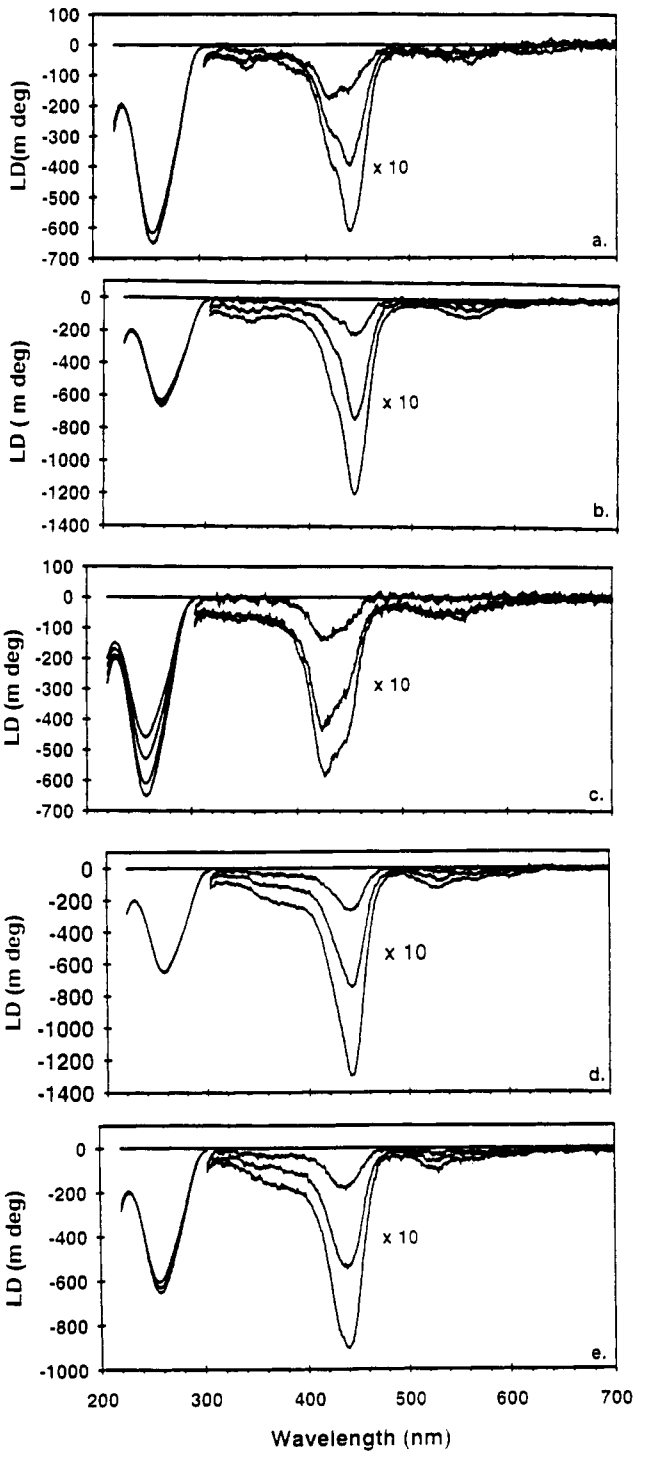

FIGURE 4: LD spectra of CoTMPyP (a), CoTBPyP (b), CoTOPyP (c), H_2TMPyP (d), and H_2TBPyP (e) complexed to CT DNA. All concentrations are the same as in Figure 2. Flow speed is 600 rpm, and optical path length is 10 mm.

geometry that excludes intercalation. A significant decrease in LD^r values in the 220–300-nm region upon addition of the cobalt porphyrins (Figure 5a–c) suggests that the ability of the DNA molecules to orient along the flow lines is decreased upon binding to these porphyrins.

Fluorescence Energy Transfer. Contact energy transfer from nucleic acid bases to bound porphyrins was measured from fluorescence excitation spectra recorded between 220 and 310 nm. Since energy transfer can only occur if a ligand closely contacts the DNA bases, the technique is often used as a criterion for intercalation (Reinhardt *et al.*, 1982). Such energy-transfer experiments were performed with all the porphyrins studied. The three cobalt porphyrins did not show energy transfer from DNA bases (curve A in Figure 6), while H_2TMPyP and H_2TBPyP increased the fluroescence quantum yield by a factor of 1.6 and 2.2, respectively (curves B and C in Figure 6), in the DNA absorption region, indicating that significant energy is transferred from excited DNA bases to the ligands.

Cleavage Kinetics of the Cobalt Porphyrins. The corrected spot intensities as described in the Materials and Methods section were fitted to eq 1 and 2 by searching for the values of the four parameters which minimized the sum of the squared deviations between the normalized intensities and the theo-

Table 1: Linear Dichroism Analysis

complex	effective transition moment angle (α)	plane orientation[a] (β)
H_2TMPyP–DNA	85 ± 5°	82°
H_2TBPyP–DNA	75 ± 5°	69°
CoTMPyP–DNA	58 ± 1°	42°
CoTBPy–DNA	60 ± 1°	45°
CoTOPyP–DNA	59 ± 1°	43°

[a] Assuming effectively degenerate polarizations of the transition dipoles in the molecular plane.

retical expressions. The resulting values for the parameters, including the root mean square deviation between theoretical and experimental for all three cobalt porphyrins, are given in Table 2. The normalized spot intensities are shown in Figure 8a–c, together with the values of the theoretical expressions using these parameters.

DISCUSSION

CD and Absorption Spectra. The free bases, H_2TMPyP and H_2TBPyP, which have no axial ligands show a substantial red-shift at the Soret maximum (Figure 2). Upon binding to CT DNA they also exhibit negative CD bands in the visible region (Figure 3). These observations indicated that the unmetallated porphyrins have strong interactions with the bases of DNA. For the cobalt porphyrins, which have axial ligands attached to the metal ion, red-shifts of 5–8 nm of the Soret maxima and rather strong, positive induced CD bands are observed in the visible region when they are complexed with CT DNA. In addition, the cobalt porphyrins display hyperchromicity or very small hypochromicity with CT DNA rather than the usual substantial hypochromism associated with intercalating molecules. By way of analogy, when proflavin intercalates into DNA, significant hypochromicity of its visible absorption band occurs, unlike the nonintercalating derivative 2,7-di-*tert*-butylproflavin which displays significant hyperchromicity (Müller *et al.*, 1973). The diaxially liganded metalloporphyrins have a ligand–metal–ligand distance of approximately 7–10 Å. ZnTMPyP, which is 5 coordinate and does not intercalate (Pasternack *et al.*, 1983), has an approximate "thickness" of 5 Å (Hoard, 1975). Since the spacing between base pairs adjacent to an intercalated ligand is ~6.8 Å, cationic metalloporphyrin possessing even one axial group is too thick for intercalation into DNA.

LD and LD^r of H_2TMPyP and H_2TBPyP. The values of LD of the H_2TMPyP–DNA complex are the same as those for DNA alone in the 260-nm region (Figure 4d). Therefore, this porphryin does not contribute significantly to the linear dichroism of the complex at ~260 nm; suggesting that the pyridyl groups, which absorb significantly in this wavelength range, are characterized by either a low degree of orientation or orientation angles of ~55° (the angle at which LD is ~0, eq 6). The LD for the H_2TBPyP complex is somewhat lower than for DNA alone in the 260-nm region (Figure 4), indicating some positive contribution of the DNA helix, probably from the bound porphyrin.

For the H_2TMPyP–DNA and H_2TBPyP–DNA complexes, the linear dichroism maxima within the 440-nm Soret band and within the 525–530-nm absorption band are slightly red-shifted (by 4 nm) with respect to the absorption maxima. Because of this, the reduced linear dichroism is not constant as a function of the wavelength is the visible region of the spectrum. Assuming that the average angle between the base pairs and the DNA helix axis is 86° (Matsuoka & Nordén, 1982, 1983), the average angles of the transition moment

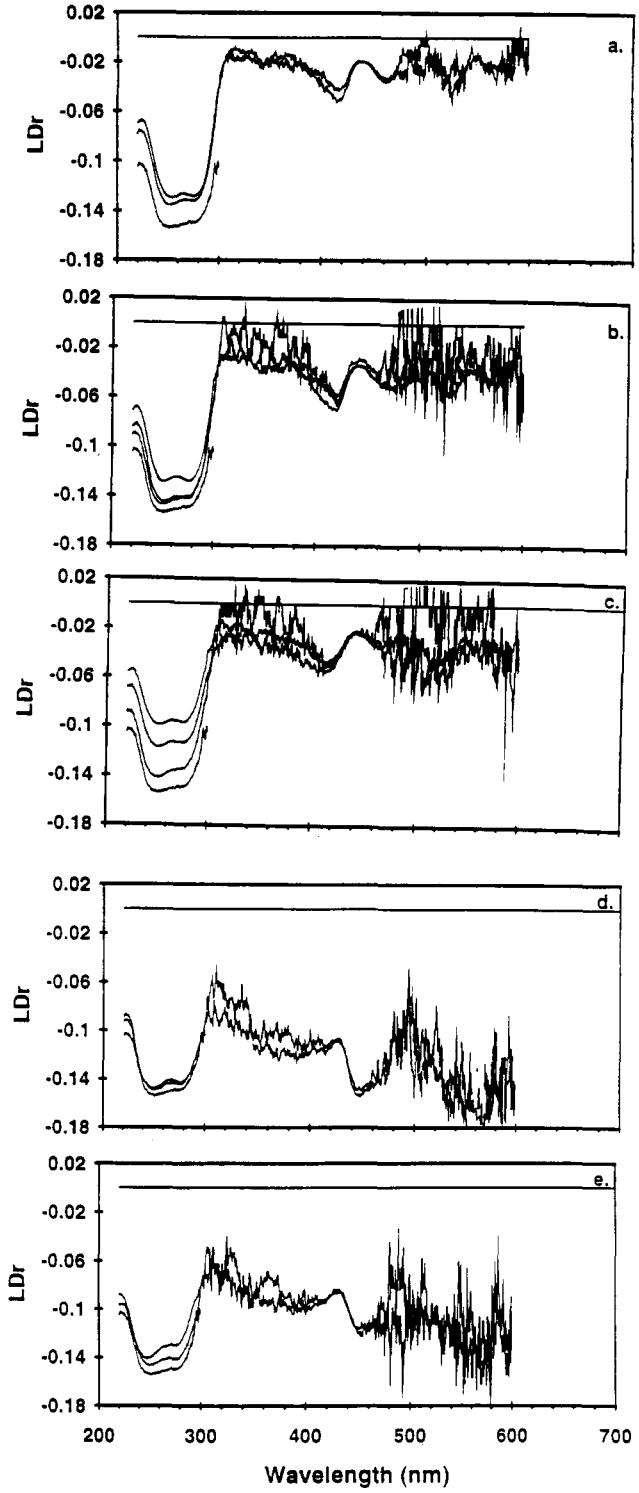

FIGURE 5: Spectra of the reduced linear dichroism of DNA complexed to CoTMPyP (a), CoTBPyP (b), CoTOPyP (c), H_2TMPyP (d), and H_2TBPyP (e). LD^r is calculated according to eq 7. In the figure, the R values for (b) and (c) are the same as in Figure 2. The R values for (a), (d), and (e) are 0.000, 0.006, and 0.010. The CT DNA concentration is 100 μM.

around the Soret maximum can be calculated according to eq 6 as 85 ± 1° and 75 ± 1° for H_2TMPyP–DNA and H_2TBPyP–DNA, respectively. The angles calculated from all ratios of porphyrin to DNA fall into the same range, suggesting homogeneous binding mode for the two unmetallated porphyrins with CT DNA. Also, the values of the angles strongly indicate that both H_2TMPyP and H_2TBPyP bind by intercalation to DNA. A clear difference in the LD^r values for x

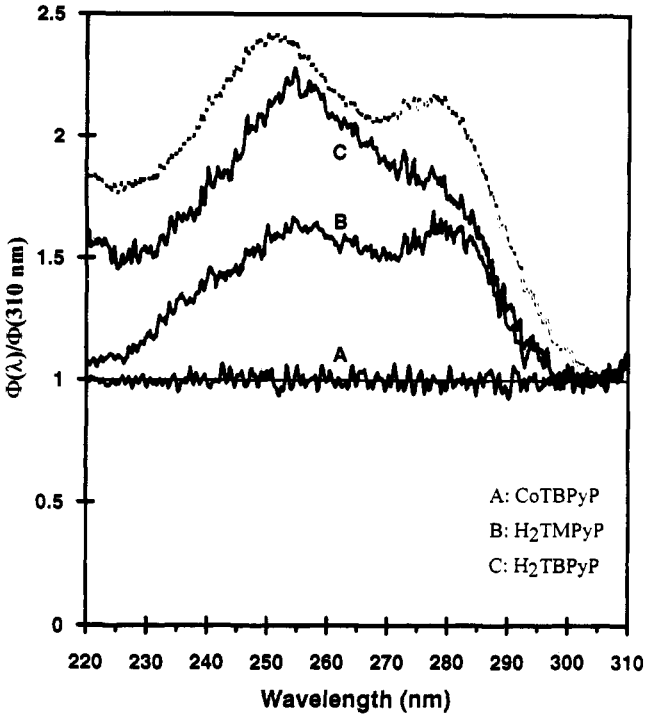

FIGURE 6: Energy transfer from DNA bases to CoTBPyP (A), H_2-TMPyP (B), and H_2TBPyP (C). For comparison the ratio $(A_{DNA} + A_{dye})/A_{dye}$ is shown (dotted curve); A_{DNA} and A_{dye}, respectively, denoting the absorbance spectra of DNA and bound dye. The CT DNA concentration is 10 μM, and the concentration of the porphyrins is 1 μM. Emission wavelength was 660 nm (bandpass 40 nm). Excitation bandpass was 4 nm, and the optical path length was 10 nm.

and y transition moments, therefore, indicates that these transition moments have somewhat different angles relative to the DNA helix axis.

The absorption band above 500 nm is oriented along the y direction of the ring system, while the Soret band is characterized by a mixed x and y polarization (Weiss, 1972). The generally high values of the reduced linear dichroism in the 400–600-nm range support the previous conclusion, based on the LD^r values observed within the Soret band, that the orientation of the planes of the two porphyrin ring systems are parallel or nearly parallel to the planes of the DNA bases.

LD and LD^r of the Cobalt Porphyrins. The magnitudes of the LD signals are only slightly smaller than that of DNA alone in the 260-nm region, except for CoTOPyP which decreases the LD signal significantly compared to that of free DNA (Figure 4a–c). The decrease in magnitude can be explained by external binding in such a way so as to increase the flexibility of DNA. In the Soret band region, in contrast to H_2TMPyP–DNA and H_2TBPyP–DNA, the reduced linear dichroism is about 70% smaller than that of the DNA region (Figure 4a–c). Furthermore, the LD^r values are not constant across this absorption band, suggesting that the x and y directions of the porphyrin ring systems with respect to the planes of the DNA bases are somewhat different. On the basis of eq 6, and with methods outlined elsewhere (Nordén & Tjerneld, 1976; Nordén *et al.* 1992), orientation angles of the porphyrin transition moments relative to the DNA helix axis can be calculated. Assuming a tilt angle of the DNA bases relative to this axis of 86°, porphyrin orientation angles of 62 ± 1°, 65 ± 1°, 64 ± 1° (utilizing LD^r values in the 400–420-nm range) and 58 ± 1°, 60 ± 1°, 59 ± 1° (utilizing the reduced dichroism values in the 420–460-nm range) are obtained for CoTMPyP, CoTBPyP, and CoTOPyP, respectively.

In summary, the planes of the metalloporphyrin derivatives studied are oriented at angles of roughly 45° with respect to the axis of DNA. This conclusion is reinforced by the LD^r values obtained for the y-polarized transitions in the 550–570-nm range; the reduced linear dichroism in this wavelength range is similar in magnitudes to the values determined within the Soret band. The calculated orientation angles of the complexed metalloporphyrin molecules are clearly inconsistent with those of intercalation complexes and in agreement with earlier conclusions that similar molecules are bound to DNA in an externally binding mode (Fiel *et al.*, 1979; Carvlin & Fiel, 1983; Carvlin *et al.*, 1983; Pasternack *et al.*, 1983; Geacintov *et al.*, 1987). In light of the increased flexibility indicated by the difficulty in orienting DNA (decreased S value), it is possible that the porphyrins are end-on bound in a partially melted region of DNA. The orientation of the chromophore is also consistent with groove binding (Nordén *et al.*, 1992).

Energy Transfer. Porphyrins that contact closely with DNA bases are characterized by clear increases of their fluorescence quantum yields for an excitation around 260 nm corresponding to an energy transfer from DNA bases to the porphyrins (Sari *et al.*, 1990). Such an energy transfer was obtained for the two unmetallated porphyrins examined here. The fluorescence quantum yield was increased by a factor of 1.6 for H_2TMPyP and 2.2 for H_2TBPyP (Figure 6), while none of the metalloporphyrin derivatives gave any increase in the quantum yield. From this observation, the conclusion can be drawn that both H_2TMPyP and H_2TBPyP are in close contact with the DNA bases whereas neither CoTMPyP, CoTBPyP, nor CoTOPyP show such a behavior.

As is shown in Figure 7, the cobalt porphyrins, in the presence of $KHSO_5$, can cleave PM2 DNA. The mechanism by which this occurs is not clear, but extensive work by Groves and co-workers (Groves, 1979; Groves *et al.*, 1983a,b) has shown that, in non-aqueous media, iron and manganese porphyrins can be oxidized with iodosobenzene or superoxide to higher valent oxo species having a ligated oxygen atom. In the presence of alkanes or olefins, the coordinated oxygen atom can be inserted into C-H and C=C bonds to form alcohols and epoxides, respectively. Little is known about the activation chemistry of cationic cobalt porphyrins, but CoTMPyP has been reported to exhibit superoxide dismutase activity in water (Peretz *et al.*, 1982).

The inspection of Figure 7 and the kinetic analysis of the cleavage data reveal that all three cobalt porphyrins are single-strand cleavage agents, *i.e.*, a single activation event on the porphyrin leads to a break in one of the DNA strands. In this respect, the compounds are similar to the DNA hydrolytic enzyme DNase I and the anticancer agent esperamicin A_1 (Kishikawa, 1991). Analogy with MnTMPyP/$KHSO_5$ (Pitié *et al.*, 1992; Prativel *et al.*, 1991), suggests that DNA breakage by the cobalt porphyrins probably involves oxygen insertion from a high valent oxo species, ultimately resulting in a strand break. No evidence was found that the cobalt porphyrins participate in a double-strand cleavage process. This would require an initial break on one strand followed quickly by a second break on the opposing strand. The overall process, effectively a double-strand or "simultaneous" cleavage event, would cause form I DNA to be converted directly to form III DNA. This is in fact the case for the anticancer drug calicheamicin, which proceeds through a phenylene diradical intermediate in causing a double-strand break in DNA (Kishikawa, 1991).

Table 2: Parameters Derived by Fitting Measured Intensities

compound	parameter						
	C_0[a]	N_0[a]	L_0[a]	k_1'	k_2'	k_3'	D
CoTMPyP	728	229	0	0.0386 ± 0.0029	(8 ± 8) × 10^{-5}		16
CoTBPyP	1042	336	0	0.0283 ± 0.0024	(9 ± 9) × 10^{-5}		31
CoTOPyP	1301	524	59	0.0127 ± 0.0015	(6 ± 5) × 10^{-4}	(6 ± 6) × 10^{-4}	31

[a] All in arbitrary units. C_0, initial concentration of form I DNA; N_0, initial concentration of form II DNA; L_0, initial concentration of linear DNA; k_1', rate constant associated with form I → form II; k_2', rate constant associated with form II → form III; k_3', rate constant associated with form III → products. Units of rate constants are μM^{-1} min^{-1}. The quantity D is the root mean square deviation between experimental and calculated data. Stated errors are changes producing 10% increase in D^2.

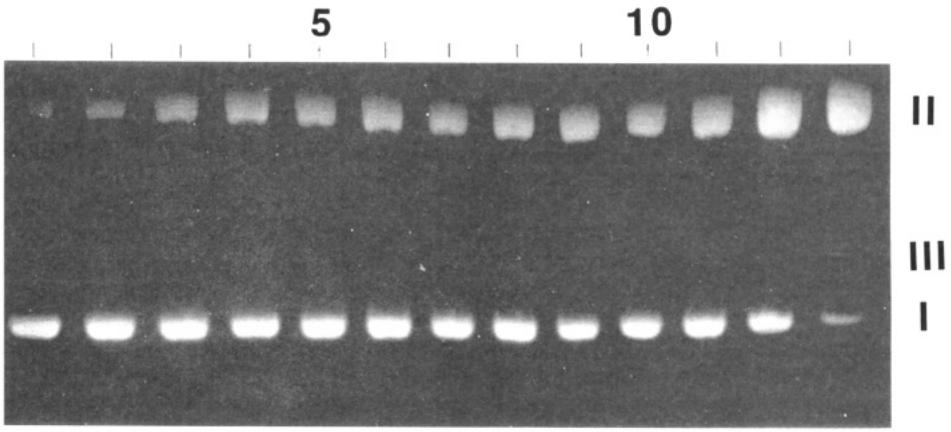

FIGURE 7: **Agarose gel showing cleavage of PM2 DNA by CoTMPyP. The symbols I, II, and III refer to form I, closed circular; form II, nicked circular; and form III, linear DNA, respectively.** The concentration of porphyrin in the lanes, which increases left to right, and the conditions of the cleavage experiments are given in the Materials and Methods section. The gels resulting from the cleavage of PM2 DNA by CoTMPyP and CoTOPyP were of quality comparable to that shown in the figure.

The apparent cleavage rates for the conversion of form I DNA to form II DNA, k_1', in Table 2 are about an order of magnitude larger than those observed for esperamicin A_1, a k_1' of 1.95 (Kishikawa, 1991). Without knowledge of the binding constants for the drug and the porphyrins, it is difficult to determine if the rate differences are due to differences in cleavage rate constants or differences in affinities of the agents for DNA. Despite literature reports that binding constants for porphyrin–DNA interactions are measurable (Strickland *et al.*, 1990), efforts to determine the DNA affinities of the cobalt porphyrins were unsuccessful. Centrifugation of solutions containing 5 μM CoTMPyP caused the absorbance of the solution to decrease by ~20%. This observation, which is consistent with aggregation, complicated attempts to analyze the optical data via Scatchard methods. The LD studies show that all three porphyrins have the same orientation relative to the DNA helix axis. This observation strongly suggests that the disposition between the activated porphyrin and its DNA target is similar for all three compounds and that the observed differences in cleavage rates (Table 2) are due to differences in affinities rather than differences in cleavage rate constants.

The binding model which emerges from these studies confirms earlier views of the porphyrin DNA interaction. The fact that the unmetallated porphyrins, H_2TMPyP and H_2TBPyP, intercalate shows that the length of the alkyl chain does not affect the insertion of the porphyrin plane between the base pairs of DNA. The mechanism by which this occurs is not understood, but the size of the substituent groups and the dimensions of the porphyrin strongly suggest that hydrogen-bonding and stacking forces involving the bases of DNA are disrupted as insertion occurs. The resulting complex is stabilized by favorable electrostatic interactions between the alkylated pyridine nitrogen atoms and the negatively charged phosphate groups of DNA. Additional stabilization is provided by van der Waals contacts (stacking interactions) between the porphyrin core and the base pairs at the intercalation site. The role of water in stabilizing the complex is also important since intercalation effectively "hides" the hydrophobic core of the porphyrin from solvent.

Outside-binding porphyrins are believed to interact in the minor groove of DNA (Pratviel *et al.*, 1991; Dabrowiak *et al.*, 1989; Hui *et al.*, 1990; Fiel, 1989; Marzilli, 1990; Gibbs & Pasternack, 1989). Although many structural details are lacking, a number of factors indicate that DNA may be distorted at the porphyrin binding site. As was earlier mentioned, the DNA molecules are difficult to orient when bound to the cobalt complexes shown in Figure 1. Difficulty in orienting was also noted by Geacintov *et al.* (1987) in studies with the outside-binding porphyrin ZnTMPyP. These workers concluded that the compound is bound to a site which is bent, kinked, or possesses some type of open structure. Similar observations have been made for $\Delta Ru(phen)_3^{2+}$ which kinks DNA (Satyanarayana *et al.*, 1992, 1993) and reduces the ability of DNA to orient in flow dichroism experiments (Hiort *et al.*, 1990). Studies involving rod-like DNA and ZnTMPyP, a porphyrin which binds in an outside manner to DNA (Marzilli, 1990), show that the viscosity of solutions decrease as ligand binding occurs (Banville *et al.*, 1983). This effect is the same as that observed for several aromatic substituted diammonium cations (Kopicak & Gabby, 1975), $\Delta Ru(phen)_3^{2+}$ (Satyanarayana *et al.*, 1992, 1993) and the propeller-shaped dye, crystal violet (Wakelin *et al.*, 1981), all of which are believed to kink DNA. The kink is caused by *partial* insertion of a ligand group between the base pairs of DNA. In view of the structures of the non-intercalating porphyrins and the angle that they make with the helix axis (~45°), it is difficult to see how they could kink DNA through partial intercalation. Axial ligands on the metal ion block intercalation of the porphyrin core while the substituents on the

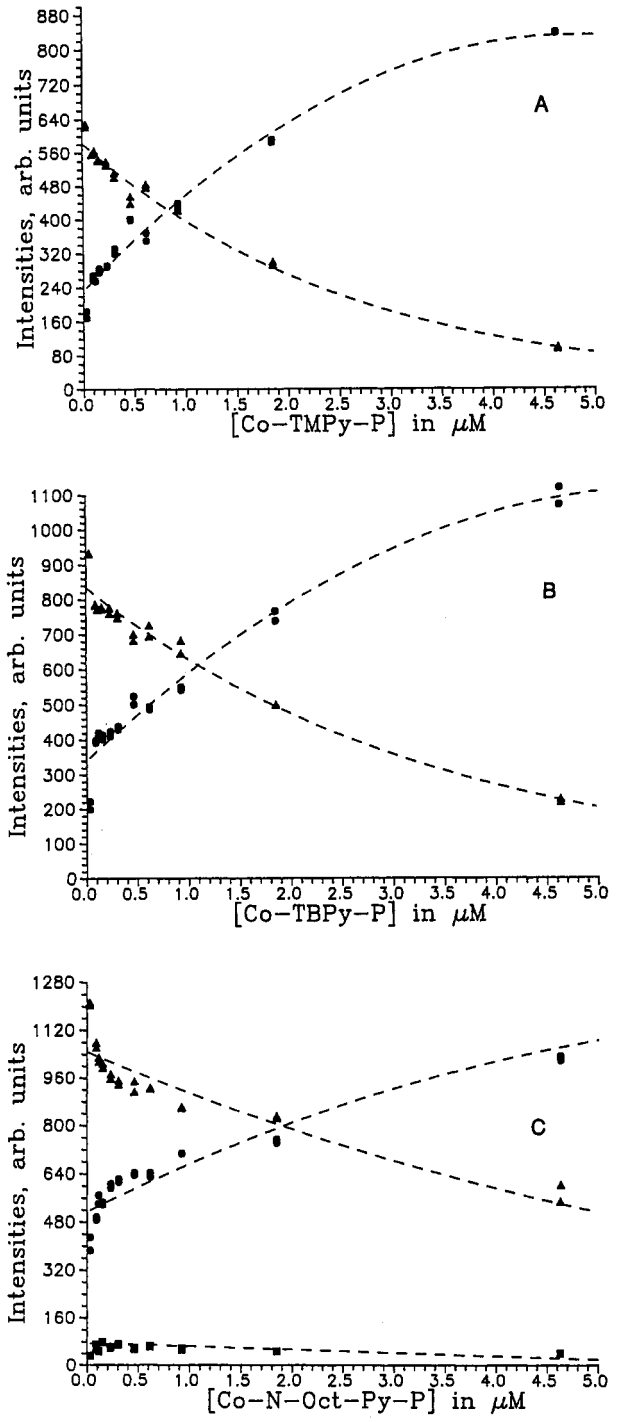

FIGURE 8: Plots of intensity (form I–III DNA) versus porphyrin concentration for CoTMPyP (a), CoTBPyP (b), and CoTOPyP (c). The observed intensities, after normalization (Materials and Methods), and the calculated curves are shown.

alkylated pyridine nitrogen atoms prevent insertion of one of the pyridine groups between the base pairs of DNA. One would expect that if the alkylated pyridine groups were important in determining the structure of the resulting complex, increasing the length of the alkyl substituent on the pyridine would influence the binding geometry. This is clearly not the case for the three cobalt porphyrin complexes studied, all of which make approximately the same angle with the DNA helix axis. Perhaps a more reasonable view is that the organization of DNA is disrupted at the site of binding. If, for example, the hydrogen bonds between adenine and thymine are broken, the steric demands imposed by the substituents on the pyridine groups would be greatly reduced. This would allow "inclusion" of the porphyrin into a partially melted region of DNA. This model, which was earlier used to explain the identical DNA cleavage patterns of cationic manganese porphyrins having different substituents on the alkylated pyridine groups (Raner *et al.*, 1988), is also consistent with the elegant mechanistic work of Bernadou and Meunier and their co-workers (Pitié, 1992) on porphyrin cleavage of DNA. The latter work showed that the activated oxo intermediate of MnTMPyP cleaves single-stranded polynucleotides and double-stranded calf thymus DNA by hydroxylating the anomeric carbon atom C1′ (Pratviel *et al.*, 1991; Bernadou *et al.*, 1989). For double-stranded DNA, this carbon atom is located deep within the minor groove, and without a significant distortion in DNA it is difficult to see how this site can be hydroxylated by the activated porphyrin.

While intercalation of porphyrins is analogous to the "threading" which takes place with the anticancer drug nogalamycin (Williams *et al.*, 1990), the model proposed for the outside-binding porphyrins has no precedence in the ligand–DNA literature. However, AT-rich regions are easier to melt than GC sites, and it is possible that the binding energy may be sufficient to overcome the energy loss due to the separation of Watson–Crick base pairing. In addition to favorable electrostatic interaction, the unusual mode of binding may be enhanced by the formation of π complexes between unpaired adenine and thymine residues with planar surface on the porphyrin core and pyridine groups attached to the methine carbon atoms. Clearly, additional work will be necessary to ascertain if this model is in fact correct. However, in view of the measured angle between the porphyrin plane and helix axis and the aforementioned observations, an "inclusion" type model is an attractive possibility.

REFERENCES

Banville, D. L., Marzilli, L. G., & Wilson, W. D. (1983) *Biochem. Biophys. Res. Commun. 113*, 148–154.

Bauer, W., & Vinograd, J. (1968) *J. Mol. Biol. 33*, 141–171.

Berg, H., Gollnick, F. A., Triebel, H., Bauer, E., Horn, G., Fleming, J., & Kittler, L. (1978) *Bioelectrochem. Bioenerg. 5*, 335–346.

Bernadou, J., Lauretta, B., Pratviel, G., & Meunier, B. (1989) *C. R. Acad. Sci., Ser. 3 309*, 409–414.

Carvlin, M. J., & Fiel, R. J. (1983) *Nucleic Acids Res. 11*, 6121–6139.

Carvlin, M. J., Mark, E., Fiel, R. J., & Howard, J. C. (1983) *Nucleic Acids Res. 11*, 6141–6154.

Dabrowiak, J. C., Ward, B., & Goodisman, J. (1989) *Biochemistry 28*, 3314–3322.

Dalgleish, D. G., Fujita, H., & Peacocke, A. R. (1969) *Biopolymers 8*, 633–345.

Dalgleish, D. G., Fiel, M. C., & Peacocke, A. R. (1972) *Biopolymers 11*, 2415–2427.

Diamond, I., Goanelli, S. G., & McDonagh, A. F. (1977) *Biochem. Med. 17*, 121–127.

Fiel, R. J. (1989) *J. Biomol. Struct. Dyn. 6*, 1259–1274.

Fiel, R. J., Howard, J. C., & Datta-Gupta, N. (1979) *Nucleic Acids Res. 6*, 3093–3118.

Fiel, R. J., Datta-Gupta, N., Mark, E. H., & Howard, J. C. (1981) *Cancer Res. 41*, 3543–3545.

Fiel, R. J., Beerman, T. A., Mark, E. H., & Datta-Gupta, N. (1982) *Biochem. Biophys. Res. Commun. 107*, 1067–1074.

Ford, K. G., Pearl, L. H., & Neidle, S. (1987) *Nucleic Acids Res. 15*, 6553–6562.

Fouquet, E., Pratviel, G., Bernadou, J., & Meunier, B. (1987) *J. Chem. Soc. Chem. Commun.* 1169–1170.

Gasmi, G., Pasdeloup, M., Pratviel, G., Pitié, M., Bernadou, J., & Meunier, J. (1991) *Nucleic Acids Res. 19*, 2835.

Geacintov, N. E., Ibanez, V., Rougee, M., & Bemsasson, R. V. (1987) *Biochemistry 26*, 3087–3092.
Gibbs, E. J., & Pasternack, R. F. (1989) *Semin. Hematol. 26*, 77–85.
Groves, J. T. (1979) *Adv. Inorg. Biochem. 1*, 119–145.
Groves, J. T., & Nemo, T. E. (1983a) *J. Am. Chem. Soc. 105*, 5786–5791.
Groves, J. T., & Nemo, T. E. (1983b) *J. Am. Chem. Soc. 105*, 6243–6248.
Groves, J. T., Watanabe, J., & McMurry, T. J. (1983) *J. Am. Chem. Soc. 105*, 4489–4490.
Härd, B., & Nordén, B. (1986) *Biopolymers 25*, 1209–1228.
Hiort, C., Nordén, B., & Rodger, A. (1990) *J. Am. Chem. Soc. 97*, 403–408.
Hoard, J. L. (1975) in *Porphyrins and Metalloporphyrins* (Smith, K. M., Ed.) pp 317–380, Elsevier, Amsterdam, The Netherlands.
Hui, X., Gresh, N., & Pullman, B. (1990) *Nucleic Acids Res. 18*, 1109–1114.
Kapicak, L., & Gabbay, E. J. (1975) *J. Am. Chem. Soc. 97*, 403–408.
Kishikawa, H., Jiang, Y.-P., Goodisman, J., & Dabrowiak, J. C. (1991) *J. Am. Chem. Soc. 113*, 5434–5440.
Kuroda, R., Takahashi, E., Austin, C. A., & Fisher, L. M. (1990) *FEBS Lett. 262*, 293–298.
LePecq, J.-B., & Paoletti, C. (1967) *J. Mol. Biol. 27*, 87–106.
Marzilli, L. G. (1990) *New J. Chem. 14*, 409–420.
Marzilli, L. G., Petho, G., Lin, M., Kim, M. S., & Dixon, D. W. (1992) *J. Am. Chem. Soc. 114*, 7575–7577.
Matsuoka, Y., & Nordén, B. (1982) *Biopolymers 21*, 2433.
Matsuoka, Y., & Nordén, B. (1983) *Biopolymers 22*, 1713–1734.
Müller, W., Crothers, D. M., & Waring, M. J. (1973) *Eur. J. Biochem. 39*, 23–234.
Nordén, B., & Tjerneld, F. (1976) *Biophys. Chem. 4*, 191–198.
Nordén, B., & Seth, S. (1985) *Appl. Spectrosc. 39*, 647–655.
Nordén, B., Kubista, M., & Kurucsev, T. (1992) *Q. Rev. Biophys. 25*, 51–170.
Pasternack, R. F., & Gibbs, E. J. (1989) *Metal DNA Chemistry* (Tullius, T., Ed.) pp 59–73, American Chemical Society, Washington, DC.
Pasternack, R. F., Gibbs, E. J., & Villafranca, J. J. (1983) *Biochemistry 22*, 2406–2414.
Peretz, P., Soloman, D., Weinraub, O., & Farraggi, M. (1982) *Int. J. Radiat. Biol. Relat. Stud. Phys., Chem. Med. 42*, 449–456.
Pitié, M., Pratviel, G., Bernadou, J., & Meunier, B. (1992) *Proc. Natl. Acad. Sci. U.S.A. 84*, 3967–3971.
Praseuth, D., Gaudemer, A., Verlhac, J.-B., Kralic, I., Sissoëff, I., & Guillé, E. (1986) *Photochem. Photobiol. 44*, 717–724.
Pratviel, G., Bernadou, J., Ricci, M., & Meunier, B. (1989) *Biochem. Biophys. Res. Commun. 160*, 1212–1218.
Pratviel, G., Pitié, M., Bernadou, J., & Meunier, B. (1991) *Nucleic Acids Res. 19*, 6283–6288.
Raner, G., Ward, B., & Dabrowiak, J. C. (1988) *J. Coord. Chem. 19*, 17–23.
Raner, G., Goodisman, J., & Dabrowiak, J. C. (1989) *Metal-DNA Chemistry* (Tullius, T., Ed.) pp 74–89, American Chemical Society, Washington, DC.
Reinhardt, C. G., Roques, B. P., & LePecq, J. B. (1982) *Biochem. Biophys. Res. Commun. 104*, 1376–1385.
Sari, M. A., Battioni, J. P., Dupré, D., Mansuy, D., & Le Pecq, J. B. (1990) *Biochemistry 29*, 4205–4215.
Satyanarayana, S., Dabrowiak, J. C., & Chaires, J. B. (1992) *Biochemistry 31*, 9319–9324.
Satyanarayana, S., Dabrowiak, J. C., & Chaires, J. B. (1993) *Biochemistry 32*, 2573–2584.
Strickland, J. A., Marzilli, L. G., & Wilson, W. D. (1990) *Biopolymers 29*, 1307–1323.
Wada, A., & Kozawa, S. (1964) *J. Polym. Sci. A2*, 853–864.
Wakelin, L. P. G., Adams, A., Hunter, C., & Waring, M. J. (1981) *Biochemistry 20*, 5779–5787.
Ward, B., Skorobogaty, A., & Dabrowiak, J. C. (1986a) *Biochemistry 25*, 7827–7833.
Ward, B., Skorobogaty, A., & Dabrowiak, J. C. (1986b) *Biochemistry 25*, 6875–6883.
Weiss, C. (1972) *J. Mol. Spectrosc. 44*, 37–80.
Williams, L. D., Egli, M., Gao, Q., Bash, P., van der Marel, J. G., van Boom, J. H., Rich, A., & Frederick, C. A. (1990) *Proc. Natl. Acad. Sci. U.S.A. 87*, 2225–2229.